Bachelor's Thesis

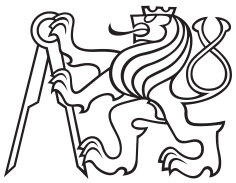

Czech Technical University in Prague

F3

Faculty of Electrical Engineering
Department of Radioelectronics

Condenser Microphone with Sigma-Delta Conversion

Antonín Gazda

Supervisor: Ing. Petr Honzík, Ph.D.
Field of study: Electronics and Communications
May 2023

BACHELOR‘S THESIS ASSIGNMENT

I. Personal and study details

Student's name: **Gazda Antonín** Personal ID number: **499215**

Faculty / Institute: **Faculty of Electrical Engineering**

Department / Institute: **Department of Radioelectronics**

Study program: **Electronics and Communications**

II. Bachelor’s thesis details

Bachelor’s thesis title in English:

Condenser Microphone with Sigma-Delta Conversion

Bachelor’s thesis title in Czech:

Kondenzátorový mikrofon se Sigma-Delta převodem

Guidelines:

Get familiar with the principles of condenser microphones and the basics of their theoretical description. Explore the principles of Sigma-Delta conversion. Implement a model of condenser microphone using an equivalent circuit. Include this model in the Sigma-Delta modulator model. Design an electronic circuit to realize the system, perform test measurements and evaluate the performance of the system.

Bibliography / sources:

[1] Škvor, Z.: Elektroakustika a akustika, ČVUT, Praha, 2012
[2] Kadlec, F.: Zpracování akustických signálů, ČVUT, Praha, 2002

Name and workplace of bachelor’s thesis supervisor:

Ing. Petr Honzík, Ph.D. Department of Radioelectronics FEE

Name and workplace of second bachelor’s thesis supervisor or consultant:

Date of bachelor’s thesis assignment: **13.02.2023** Deadline for bachelor thesis submission: **26.05.2023**

Assignment valid until: **22.09.2024**

Ing. Petr Honzík, Ph.D.	doc. Ing. Stanislav Vítek, Ph.D.	prof. Mgr. Petr Páta, Ph.D.
Supervisor’s signature	Head of department’s signature	Dean’s signature

III. Assignment receipt

The student acknowledges that the bachelor’s thesis is an individual work. The student must produce his thesis without the assistance of others, with the exception of provided consultations. Within the bachelor’s thesis, the author must state the names of consultants and include a list of references.

Date of assignment receipt	Student’s signature

© ČVUT v Praze, Design: ČVUT v Praze, VIC

Acknowledgements

I would like to thank my supervisor Ing. Petr Honzík, Ph.D. for his guidance. My thanks also go to doc. Ing. Stanislav Vítek, Ph.D. for his support during my studies.

Declaration

I hereby declare that the presented thesis is my own work and that I have cited all sources of information in accordance with the Guideline for adhering to ethical principles when elaborating an academic final thesis.

In Prague, 26th of May 2023

Prohlašuji, že jsem předloženou práci vypracoval samostatně a že jsem uvedl veškeré použité informační zdroje v souladu s Metodickým pokynem o dodržování etických principů při přípravě vysokoškolských závěrečných prací.

V Praze, 26. května 2023

Signature / Podpis: .....

Abstract

This thesis explores the possibility of realization of an acoustic transducer performing direct analog to digital conversion and evaluates its functionality. To achieve this, an experimental condenser microphone is included into a Sigma-Delta loop. First, an equivalent circuit of the microphone is implemented, a time domain model is created and used in a Sigma-Delta conversion loop. The thesis also discusses, implements and tests hardware design of the proposed system.

Keywords: condenser microphone, Sigma-Delta conversion, equivalent circuit modeling, hardware design

Supervisor: Ing. Petr Honzík, Ph.D.
Czech Technical University in Prague,
Technická 1902/2,
166 27 Praha 6

Abstrakt

Tato práce zkoumá možnost realizace akustického měniče provádějícího přímou analogově digitální konverzi a hodnotí jeho funkčnost. K dosažení tohoto cíle je do smyčky Sigma-Delta zapojen experimentální kondenzátorový mikrofon. Nejprve je implementován náhradní obvod mikrofonu, je vytvořen model v časové doméně a použit ve smyčce Sigma-Delta modulace. V práci je také diskutován, implementován a testován hardwarový návrh systému.

Klíčová slova: kondenzátorový mikrofon, Sigma-Delta převod, modelování pomocí náhradního obvodu, návrh hardware

Překlad názvu: Kondenzátorový mikrofon se Sigma-Delta převodem

Contents

Introduction 1

Part I
Theoretical Part

1 Electrostatic microphone 5
1.1 Condenser Microphone Modeling in the Frequency Domain 7
1.1.1 Mechanical Impedance of Membrane 9
1.1.2 Mechanical Gap Impedance . 10
1.1.3 Mechanical Impedance of a Hole in a Solid Electrode 10
1.1.4 Mechanical Cavity Impedance 10
1.1.5 Total Impedance 11
1.2 Condenser Microphone Modeling in the Time Domain 11

2 Implemented condenser microphone models 13
2.1 Impulse response modeling 15

3 Sigma-Delta Modulation 19
3.1 Conversion Noise 20
3.2 Generic Sigma-Delta model 20
3.3 Sigma-Delta conversion with a microphone model 21

Part II
Practical Part

4 Hardware Design of a PVDF Sigma - Delta Converter 27
4.1 Schematic design 27
4.1.1 Power Supply 27
4.1.2 Additional Compensating Circuit 28
4.1.3 Comparator 29
4.1.4 D-Latch 30
4.1.5 Output Circuitry 31
4.2 PCB design 32

5 Hardware Testing 35
5.1 Demodulation 35
5.2 Testing Setup 38

Conclusion 43

Bibliography 45

Appendices

A List of abbreviations 51

B Included files 53

Figures

1 Analogy of a microphone with a PVDF membrane as a Sigma-Delta difference block 1

1.1 Diagram of a condenser microphone with one hole 5
1.2 A schematic of a circuit used in electrostatic microphones 6
1.3 Photo of the a single-acting condenser microphone used in the practical part 7
1.4 Photo of a static electrode of a single-acting condenser microphone used in the practical part 7
1.5 Schematic of an equivalent circuit model of a single-acting condenser microphone 8

2.1 Frequency dependence of the magnitude (upper figures) and phase (lower figures) of the membrane mean displacement (left figures) and the sensitivity of the microphone (right figures). 14
2.2 Comparison between the results of the equivalent circuit model (blue curves) and the numerical results (red curves). 14
2.3 A graph of a modeled impulse response of a condenser microphone 15
2.4 Simulated output (red curves) and input (red curves) signals of an LTI system given the impulse response. 16
2.5 Simulated output of a microphone from a measured impulse response 16
2.6 Measured output of a microphone with exited PVDF membrane 17

3.1 First order Sigma-Delta block diagram 19
3.2 Dependency of SNR on oversampling rate and order of a Sigma-Delta modulator 20
3.3 Time diagrams in different blocks of first order Sigma-Delta modulation 21
3.4 A diagram of the microphone with a PVDF membrane in a Sigma-Delta loop 21
3.5 Time diagrams in different blocks of first order Sigma-Delta modulation with microphone model, oversampling rate of 8. 22
3.6 Time diagrams in different block of first order Sigma-Delta modulation with microphone model, oversampling rate of 64. 22

4.1 Schematic of the designed PSU . 28
4.2 Schematic of a proposed compensation circuit 29
4.3 Schematic of the used input block - an inverting amplifier 29
4.4 Schematic of a proposed comparator with hysteresis 30
4.5 Schematic of the implemented comparator block 30
4.6 Schematic of the D-Latch block . 30
4.7 D-Latch function table [20] 31
4.8 Inverting Output Amplifier Schematic Diagram 31
4.9 Top 2D view of the designed PVDF Sigma-Delta converter PCB 32
4.10 Top 3D view of the designed PVDF Sigma-Delta converter PCB with components 32
4.11 Bottom 2D view of the designed PVDF Sigma-Delta converter PCB 33
4.12 Bottor 3D view of the designed PVDF Sigma-Delta converter PCB with components 33

5.1 Photo of an EVAL-ADAU1452REVBZ Board . 35
5.2 Sigma Studio USB Connection Schematic 36
5.3 Sigma Studio Digital Microphone Schematic 36
5.4 DMIC CTRL0 Register Setup . . 37
5.5 Sigma Studio Pin Mode Setup . . 37
5.6 Demodulated signal from SPH0641LU4H-1 37

Tables

5.7 A diagram of the final testing setup 38
5.8 PVDF membrane excitation input (blue curves) and microphone analog output (yellow curves) 39
5.9 8 kHz Sampling Rate 100 Hz Sinewave Modulation - microphone output (yellow curves), acoustic pressure input (aqua curves), Sigma-Delta output (magenta curves), demodulated signal (blue curves) 40
5.10 8kHz Sampling Rate 100 Hz Sinewave Modulation Close Up - microphone output (yellow curves), acoustic pressure input (aqua curves), Sigma-Delta output (magenta curves), demodulated signal (blue curves) 40
5.11 Modeled Sigma-Delta diagram with dampened PVDF amplitude . 41
5.12 192kHz Sampling Rate 100Hz Sinewave Modulation 42
5.13 192kHz Sampling Rate 100Hz Sinewave Modulation Closeup 42

2.1 Equivalent circuit model parameters 13

Introduction

When designing well-performing measurement microphones, there are high demands on creating a microphone with a flat frequency response. Then there is also high demand on creating a Sigma-Delta ADC with good frequency characteristics to digitalize this signal.

The aim of this thesis is to experiment with another way to construct a microphone with a digital output - not by using an analog microphone with subsequent Sigma-Delta ADC, but to create an acoustic transducer performing direct analog to digital conversion.

This could be done by using a single-acting condenser microphone with a piezoplastic PVDF membrane, which would be able to be excited with a digital signal. By combining the acoustic analog signal with a negative digitally driven voltage sent into the piezoplastic membrane, a differential block of the Sigma-Delta loop could be created directly on the membrane. This is indicated in Figure 1.

Moreover, because of the frequency characteristics of a microphone, it could be used as a partial integrator. With more analog blocks regulating the integration, a loop could be created, which would allow more flexibility and cost saving when designing a microphone.

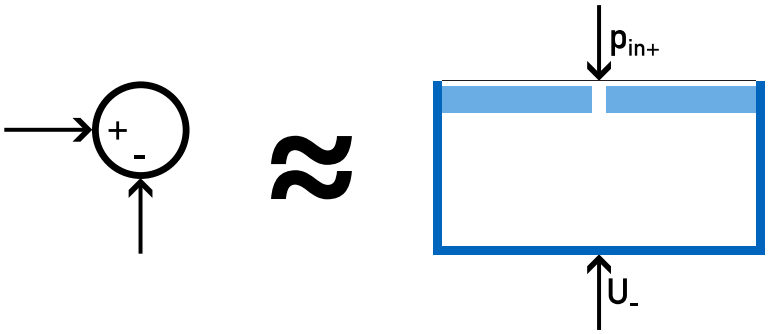

Figure 1: Analogy of a microphone with a PVDF membrane as a Sigma-Delta difference block

Part I

Theoretical Part

Chapter 1

Electrostatic microphone

Transducers are extremely important devices in acoustics and electroacoustics, which convert signal quantities of one kind into quantities of another kind [1]. An electroacoustic sensor is called a microphone. An electrostatic (or condenser) microphone is a device that converts acoustic pressure to electrical voltage.

A single-acting electrostatic microphone consists of a few notable parts:

- a static electrode with usually one or more holes
- a moving electrode - a usually tightened membrane
- an air gap between the two electrodes
- a cavity behind the static electrode

A diagram of a condenser microphone with one hole is shown in Figure 1.1.

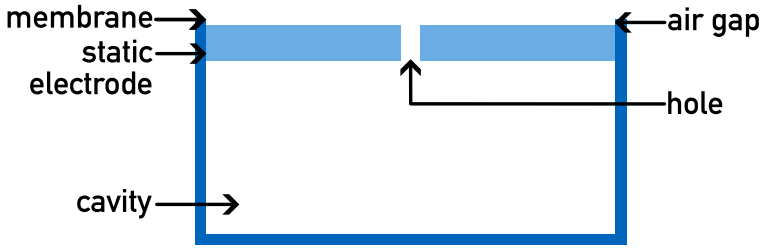

Figure 1.1: Diagram of a condenser microphone with one hole

A single-acting electrostatic microphone works on a very trivial principle. The main part of the microphone is made up of two electrodes that form a capacitor. For that applies [1]

$$C_0 = \frac{\epsilon_0 S}{h_g}, \tag{1.1}$$

where C_0 is the static capacitance, S is the electrode area, ϵ_0 is the permittivity of vacuum and h_g is the thickness of the air gap.

The total charge differential across any capacitor can be expressed as [1]

$$dQ = dCU + CdU. \tag{1.2}$$

Since almost no current flows into the charged capacitor C_0 through the resistor R_p (see Figure 1.2) of huge value (order of GΩ), it can be said that the charge of the capacitor is invariant, that is, $dQ \approx 0$. The voltage change in the capacitor depends only on the voltage caused by the movement of the membrane, that is, $dU \approx u$. The static capacitance of a capacitor is much greater than the change in capacitance when moving, i.e. $C \approx C_0$.

It follows that

$$u = -U_p \frac{C}{dC}. \tag{1.3}$$

A single-acting electrostatic microphone is created by fixing one of these electrodes, the moving electrode is called a membrane.

Since dC depends on $\overline{\xi}$ and C depends on h_g, after a simplification and linearization we get

$$u(t) = \frac{U_p \overline{\xi}}{h_g}. \tag{1.4}$$

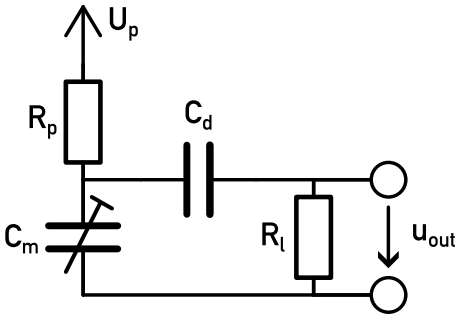

Figure 1.2: A schematic of a circuit used in electrostatic microphones

Figure 1.2 shows a simple circuit for converting a change in capacitance to a change in voltage u_{out}. The capacitor C_m is charged to the polarization voltage U_p through the resistor R_p. Polarisation voltage is typically 200V for measurement microphones. A change in capacitance will be reflected as voltage change modulated on the DC component, which is filtered out by the capacitor C_d. Therefore, at the output of this system, there is only an alternating voltage u_{out}, which is directly proportional to the change in the acoustic pressure acting on the moving membrane with an area of S.

A photo of the a condenser microphone, which was provided by the supervisor, can be seen in Figure 1.3.

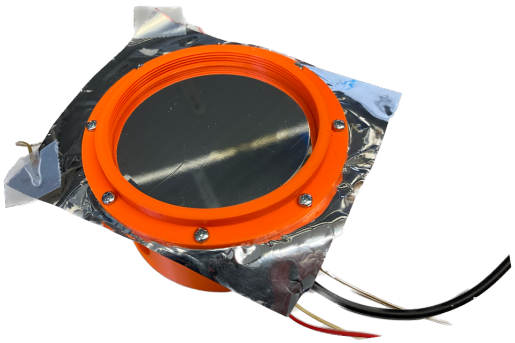

Figure 1.3: Photo of the a single-acting condenser microphone used in the practical part

A photo of the static electrode of the microphone, which is hidden under the membrane of the microphone shown in Figure 1.3, is shown in Figure 1.4.

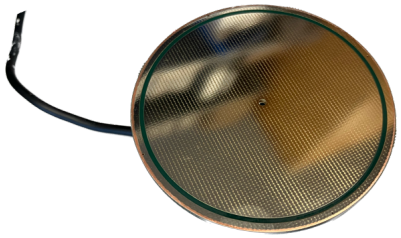

Figure 1.4: Photo of a static electrode of a single-acting condenser microphone used in the practical part

1.1 Condenser Microphone Modeling in the Frequency Domain

There are three main ways to model characteristics of a condenser microphone.

Equivalent circuit models use electroacoustic and electromechanical analogies to simulate the microphones' characteristics. They are relatively simple to understand, create and compute [5] [6] [7] [8].

Analytical models are more precise than equivalent circuit models, but require more computational power. Moreover, these models are geometrically limited [9] [10] [11].

Numerical models are of these three methods usually the most precise. They use finite element method (FEM), but are highly computationally expensive

[12] [13] [14] [15] [16].

Regarding this thesis, an equivalent circuit model was used to simulate the characteristics of a condenser microphone.

Thanks to the possibility of describing electrical, mechanical and acoustic elements in one circuit, a diagram describing an electrostatic microphone was created and can be seen in Figure 1.5.

The following content of this chapter is based on theory explained by Škvor [1] [6].

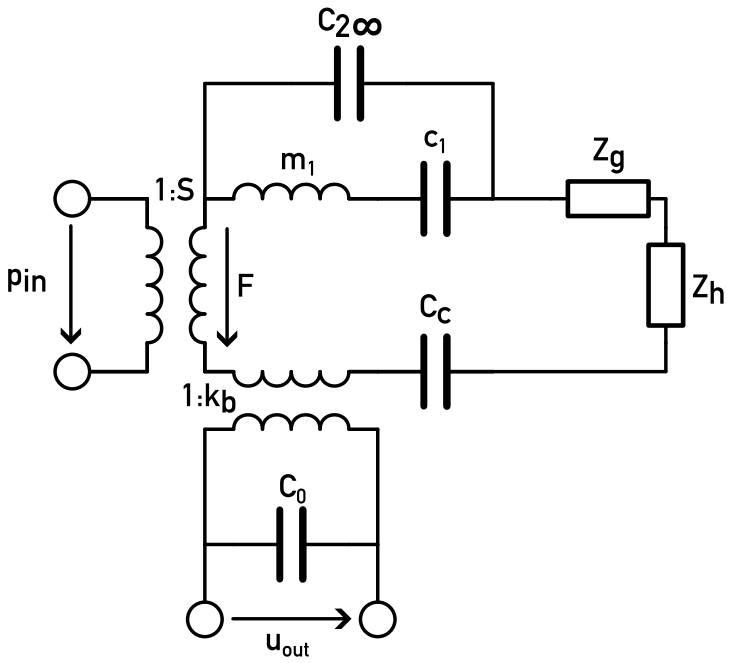

Figure 1.5: Schematic of an equivalent circuit model of a single-acting condenser microphone

This equivalent circuit consists of three main parts: acoustic, mechanical, and electrical.

The input acoustic pressure p_{in} acts on the surface of the membrane S. This transforms it into mechanical force F. The mechanical part of the circuit consists of multiple impedances, which model different mechanical parts (and acoustic parts transformed into the mechanical domain) of the microphone.

The membrane consists of mass m_1, compliance c_1, and quasi-static compliance $C_{2\infty}$. The impedance Z_g models the mechanical resistance and the mass of an air gap between the membrane and the fixed electrode. Z_h represents the mass and resistance of holes in the static electrode. The compliance C_c indicates the mechanical impedance caused by the cavity behind the static electrode.

1.1.1 Mechanical Impedance of Membrane

In the model shown in Figure 1.5, the membrane consists of M_1, C_1, $C_{2\infty}$. C_1 models the partial compliance of the membrane

$$C_1 = \frac{4}{j_1^4 \pi T}, \tag{1.5}$$

where T is the tension of the membrane and $j_1 = 2.4048$ is the first zero of the bessel function $J_0(x)$.

The inertance M_1 models the mass of the membrane

$$M_1 = \frac{j_1^4 m_1 S}{4}, \tag{1.6}$$

where $m_1 = \rho_m \cdot h_m$ is the mass per unit area and ρ_m, h_m, are density and thickness of the membrane respectively. The series connection of C_1 and M_1 then creates the first resonance frequency of the membrane.

For a more accurate calculation of the membrane, additional masses M_2 to M_n (where n goes to ∞) should also be taken into account, but in this case were neglected, as they do not affect the model significantly at low frequencies.

However, not taking into account the additional series connections M_2 to M_n and C_2 to C_n will also cause a systematic error for low frequencies since the combination of compliances C_1 to C_n gives [1]

$$C_\infty = \sum_{n=1}^{\infty} C_n = \frac{1}{8\pi T}, \tag{1.7}$$

and then [8]

$$C_{2\infty} = C_\infty - C_1. \tag{1.8}$$

The impedance based on compliance C_1 and the weight M_1 is calculated the same way as when solving electrical circuits.

$$Z_{mem_1} = \frac{1}{i\omega C_1} + i\omega M_1 \tag{1.9}$$

The impedance caused by quasi-static compliance C_∞ can be described as

$$Z_{mem_2} = \frac{1}{i\omega C_{2\infty}}. \tag{1.10}$$

The resulting membrane impedance is given by the parallel combination of impedances Z_{mem_1} and Z_{mem_2}.

$$Z_{mem} = Z_{mem_1} \parallel Z_{mem_2} = \frac{Z_{mem_1} Z_{mem_2}}{Z_{mem_1} + Z_{mem_2}} \tag{1.11}$$

1.1.2 Mechanical Gap Impedance

To determine the gap impedance, it is necessary to calculate the constant β, which is defined as [1]

$$\beta = \log \frac{r_m}{r_h} - \frac{3}{4} + \frac{r_{h^2}}{r_{m^2}} - \frac{r_{h^4}}{4 \cdot r_{m^4}}, \tag{1.12}$$

where r_m is the radius of the membrane and r_h is the radius of the hole in the static electrode.

For mechanical resistance and mass, the following equations 1.13 and 1.14 apply [1]

$$R_g = \frac{6\pi\mu r_m^4 \beta}{\pi r_h^4}, \tag{1.13}$$

$$M_g = \frac{3\pi\mu r_m^4 \beta}{\pi r_h^4}, \tag{1.14}$$

where μ is shear viscosity of the air, h_g is the thickness of the gap. The resulting gap impedance is given by [1]

$$Z_g = R_g + M_g i\omega. \tag{1.15}$$

1.1.3 Mechanical Impedance of a Hole in a Solid Electrode

The mechanical impedance of a hole in the solid electrode consists of a real component – acoustic resistance and an imaginary component – the acoustic mass of the hole. Relations 1.16 and 1.17 apply [1]

$$R_{c_{ak}} = \frac{8\mu h_e}{\pi r_h^4}, \tag{1.16}$$

$$M_{c_{ak}} = \frac{4\rho h_e}{3\pi r_h^2}, \tag{1.17}$$

where ρ is the air density, h_e is the length of the cylindrical tube - the hole in the fixed electrode. The acoustic impedance calculated in this way must be converted back into mechanical impedance by multiplying by S^2.

$$Z_g = S^2(R_{c_{ak}} + i\omega M_{c_{ak}})$$

1.1.4 Mechanical Cavity Impedance

Since it is assumed, that the radius of the membrane and the radius of the cavity S is the same,

$$V_d = Sh_d, \tag{1.18}$$

where h_d is the height of the cavity and V_d is the volume of the back cavity.

Acoustic compliance is given by relation [1]

$$C_{d_{ak}} = \frac{V_d}{\rho c^2}. \tag{1.19}$$

The mechanical impedance given by this compliance is then calculated as

$$Z_{C_d} = S^2 \frac{1}{i\omega C_d}. \tag{1.20}$$

1.1.5 Total Impedance

The total mechanical impedance of the modeled microphone is equal to the sum of all partial mechanical impedances, i.e.

$$Z_m = Z_{mem} + Z_g + Z_h + Z_c. \tag{1.21}$$

The average deflection of the microphone can then be determined from relation [1]

$$\overline{\xi} = \frac{pS}{i\omega Z_m}. \tag{1.22}$$

The sensitivity of the microphone is also calculated from the average deflection as

$$\sigma = U_0 \frac{\overline{\xi}}{p h_g}. \tag{1.23}$$

1.2 Condenser Microphone Modeling in the Time Domain

With the modeled average deflection of the microphone and the sensitivity of the microphone, it can be predicted, how the microphone will perform in the frequency domain.

If we assume that the microphone is a linear time-invariant system (LTI), an impulse response of the system describing the time domain can be obtained by applying an inverse Fourier transform.

In the frequency domain, the system can be described as

$$Y(z) = H(z)X(z), \tag{1.24}$$

where $Y(z)$ and $X(z)$ are the spectra of the output and input signal respectively. $H(z)$ is the transfer function of the system.

In the time domain, the output of the LTI can be described as

$$y(t) = h(t) * x(t), \tag{1.25}$$

where $y(t)$ is the models' output, $h(t)$ is the systems' impulse response, $*$ is convolution and $x(t)$ is the systems' input signal.

The impulse response $h(t)$ can be generated from the symmetric conjugate transfer function (sensitivity) $H(z)$ of the microphone by applying an inverse Fourier transformation.

Chapter 2

Implemented condenser microphone models

All of the condenser microphone models were implemented using the MATLAB programming language. As mentioned in chapter 1.1, an equivalent circuit was used to model the characteristics of the microphone.

Parameters, which were used in the models, are summarized in Table 2.1.

Table 2.1: Equivalent circuit model parameters

Parameter	Value	Unit	Description
p	1	Pa	pressure acting on membrane
U_p	200	V	polarization voltage
ρ_m	1944	kg/m^3	membrane density
r_m	$18 \cdot 10^{-3}$	m	membrane radius
h_m	$25 \cdot 10^{-6}$	m	membrane thickness
h_g	$230 \cdot 10^{-6}$	m	air gap thickness
r_h	$25 \cdot 10^{-6}$	m	hole radius
h_e	$1,6 \cdot 10^{-3}$	m	static electrode thickness
h_c	$7,6 \cdot 10^{-3}$	m	cavity depth
f_{res}	1040	Hz	microphones' measured resonance frequency
ρ_{air}	1,18	kg/m^3	air density
μ	$18,3 \cdot 10^{-6}$	Pa $\cdot$ s	shear dynamic air viscosity
c	345,9	m/s	speed of sound

Based on these parameters, a model of an electrostatic microphone was implemented. The MATLAB code, which also showcases how different parameters change the models' output, is included in Appendix B.

The modeled frequency dependence of the magnitude and phase of the membrane mean displacement and the sensitivity of the microphone is shown in Figure 2.1.

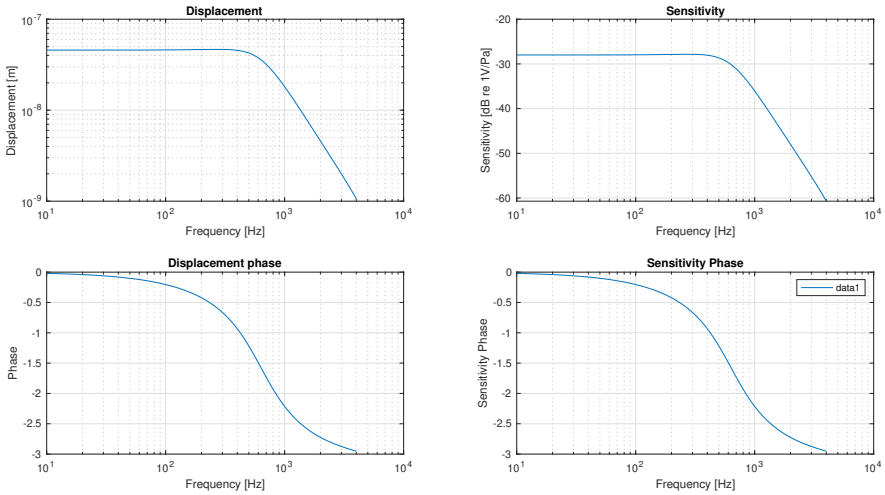

Figure 2.1: Frequency dependence of the magnitude (upper figures) and phase (lower figures) of the membrane mean displacement (left figures) and the sensitivity of the microphone (right figures).

In order to verify the precision of the equivalent circuit model, a numerical model of a microphone with exactly the same parameters as in Table 2.1 was supplied by the supervisor. This is a more accurate description of an electrostatic microphone, using the finite element method, and was calculated in the COMSOL Multiphysics Software. The results of modeled sensitivities and displacements can be seen in Figure 2.2.

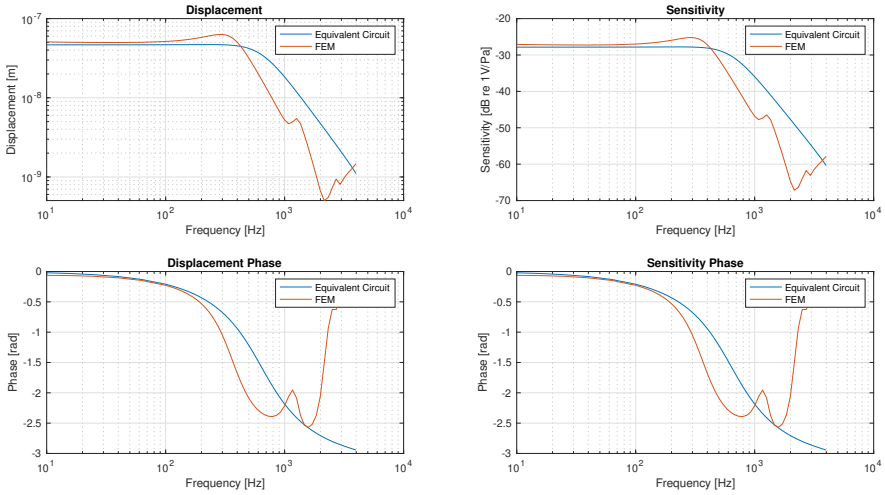

Figure 2.2: Comparison between the results of the equivalent circuit model (blue curves) and the numerical results (red curves).

It can be seen, that for low frequencies (up to 10^2 Hz) the values of both models are do not vary significantly, showing that the models differ by only

about 0.74 dB at the lowest modeled frequency of 10 Hz. The equivalent circuit model implemented in this thesis seems to be more damped.

2.1 Impulse response modeling

As indicated in Equation 1.25, an impulse response is useful for predict the output of the microphone in the time domain, given an incoming signal. A modeled impulse response can be seen in Figure 2.3.

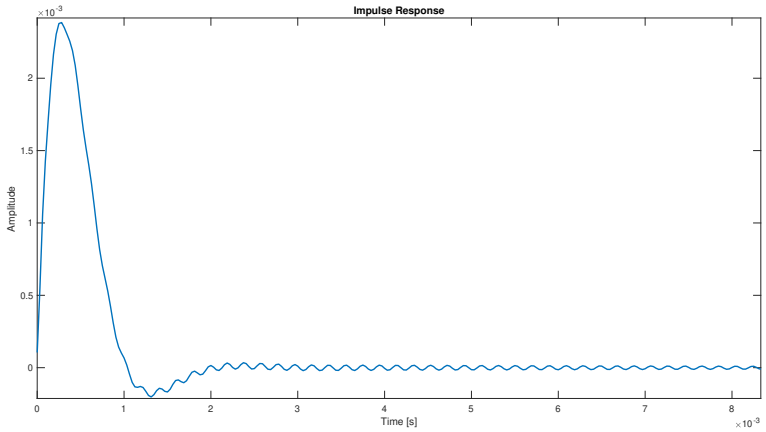

Figure 2.3: A graph of a modeled impulse response of a condenser microphone

By convolving an input signal with the impulse response according to the Equation 1.25, the output signal can be modeled. The output can be used to show, how the microphone will function in the Sigma-Delta loop.

An output signal of an LTI system given the impulse response convolved with a 200 Hz square wave of amplitude 1 was simulated and can be seen in Figure 2.4.

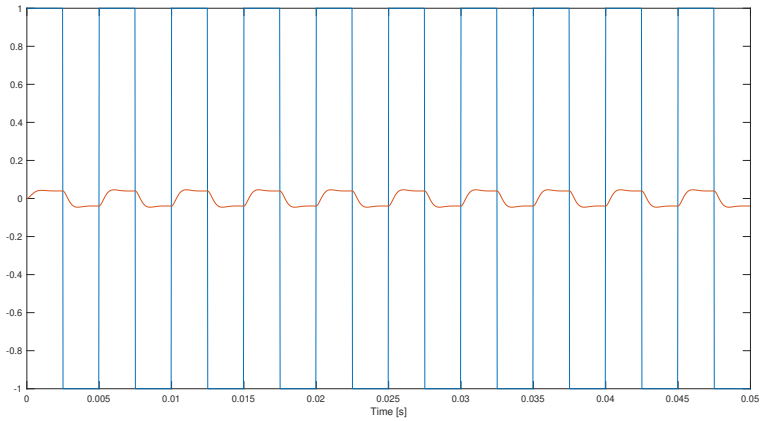

Figure 2.4: Simulated output (red curves) and input (red curves) signals of an LTI system given the impulse response.

Next, with the microphones' measured frequency characteristics, an impulse response was calculated and used in convolution with a 200 Hz square wave signal. The result of this model is displayed in Figure 2.5. Note that the response in Figure 2.4 was calculated from a V/Pa characteristic and the response in Figure 2.5 was calculated from a V/V characteristic, so the magnitude is expected to be different and there will be need of gain in further simulations.

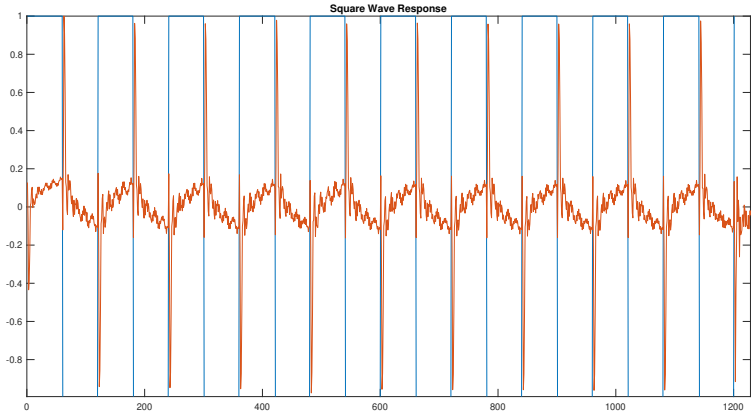

Figure 2.5: Simulated output of a microphone from a measured impulse response

Lastly - the response to sending a 200 Hz square wave signal into the PVDF membrane was measured on the experimental microphone shown in Figure 1.3 and can be seen in Figure 2.6.

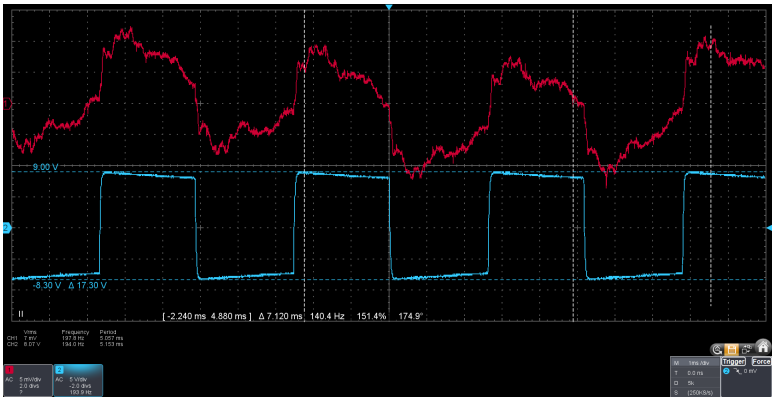

Figure 2.6: Measured output of a microphone with exited PVDF membrane

Chapter 3

Sigma-Delta Modulation

When designing any kind of system to read analog signals using a digital device, an analog to digital converter must be used (ADC).

Delta modulation is an analog-to-digital conversion method, which uses a one-bit quantizer to estimate a continuous-time signal. However, it is not suitable for high-precision applications because it is known to produce a lot of quantization noise.

Sigma-Delta modulation is a more advanced version of delta modulation, which employs a feedback loop to decrease the amount of quantization noise. This is accomplished by oversampling the input signal (usually by 64 times the sampling frequency). The resulting signal is then synchronized with an incoming clock and is fed back into the difference block through 1-bit DAC.

The feedback loop reduces quantization noise by shifting it to higher frequencies. A low-pass filter can then be used for demodulation, which also removes these components. Sigma-Delta ADCs are highly used in audio and video applications.

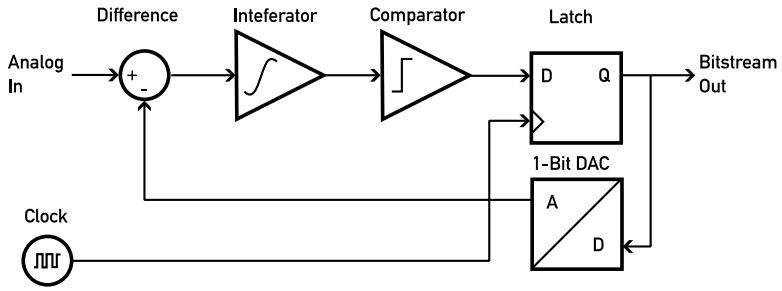

Figure 3.1: First order Sigma-Delta block diagram

A block diagram of first order Sigma-Delta modulation is shown in Figure 3.1 [4]. To summarize the functionality, the difference of the analog input and the bitstream output amplified by the 1-bit DAC gets integrated, converted into a digital signal by a comparator and then synchronized with the oversampling clock with a latch. This completes the Sigma-Delta loop.

3.1 Conversion Noise

The amount of conversion noise is based on the oversampling rate and the order of the Sigma-Delta modulator, which is demonstrated in Figure 3.2 [4].

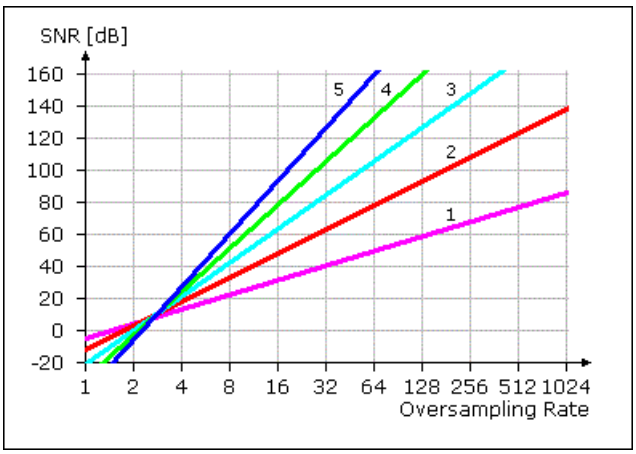

Figure 3.2: Dependency of SNR on oversampling rate and order of a Sigma-Delta modulator

3.2 Generic Sigma-Delta model

Source code written in the Python programming language for a generic Sigma-Delta modulation model was provided by the supervisor and was re-implemented into MATLAB, giving an overview of different signals in the Sigma-Delta conversion - shown in Figure 3.3. The signals were generated for a 1 kHz sinewave, 8 kHz sampling frequency and oversampling rate of 8 (i.e. clock frequency of 48 kHz).

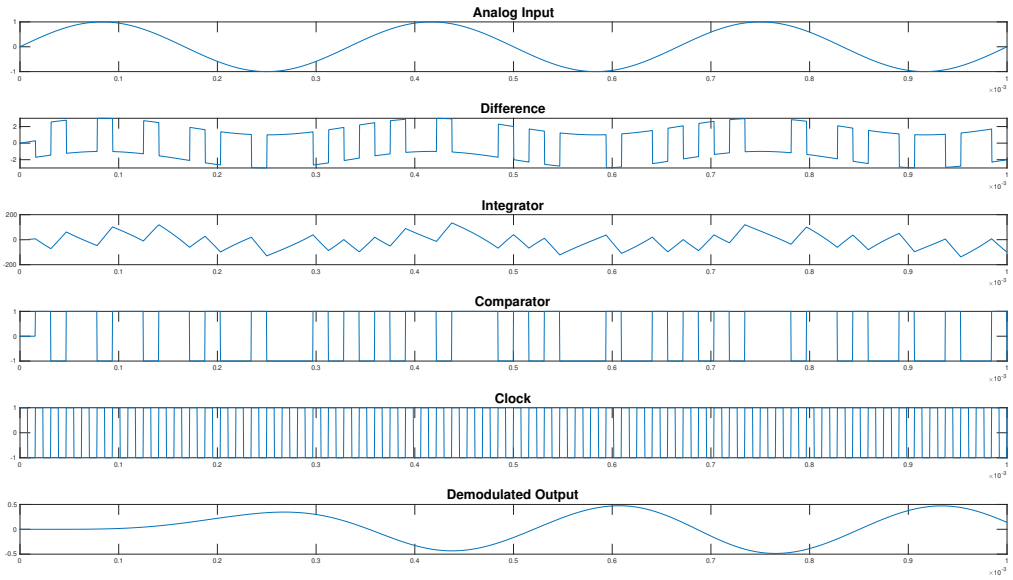

Figure 3.3: Time diagrams in different blocks of first order Sigma-Delta modulation

A diagram of a microphone with a PVDF membrane used instead of the difference and integrator block, as mentioned in the Introduction, can be seen in Figure 3.4.

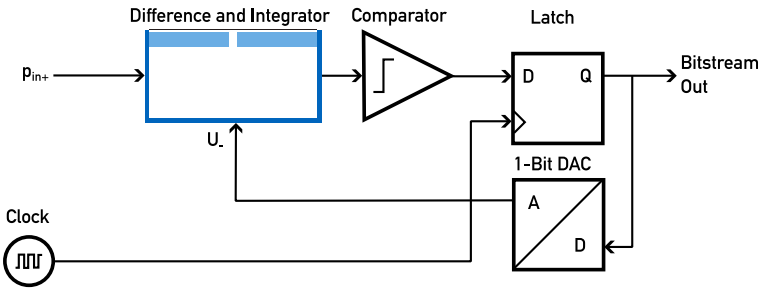

Figure 3.4: A diagram of the microphone with a PVDF membrane in a Sigma-Delta loop

3.3 Sigma-Delta conversion with a microphone model

To determine how a condenser microphone with a PVDF membrane used instead of the difference and integrator block in the Sigma-Delta conversion could work, impulse response of the modeled microphone was used in the Sigma-Delta loop simulation. Convolution was implemented in a for loop in the Sigma-Delta code, generating the Figures 3.5 and 3.6 for oversampling rates of 8 and 64 respectively.

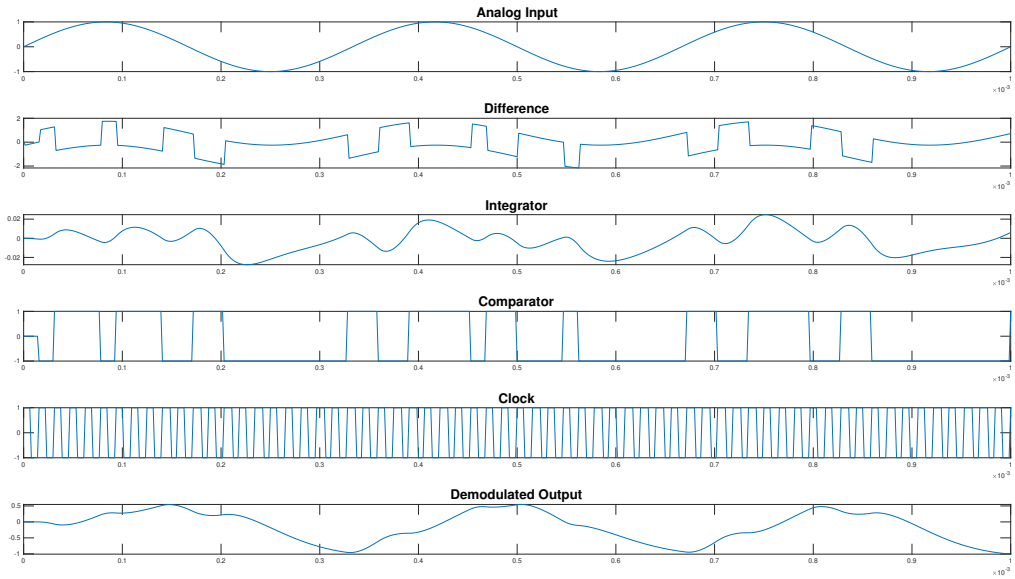

Figure 3.5: Time diagrams in different blocks of first order Sigma-Delta modulation with microphone model, oversampling rate of 8.

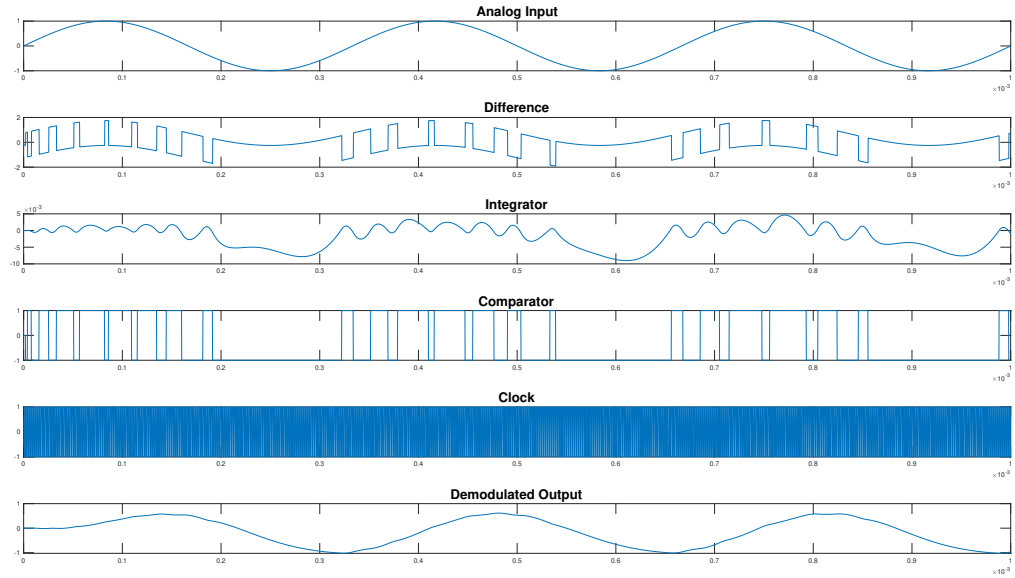

Figure 3.6: Time diagrams in different block of first order Sigma-Delta modulation with microphone model, oversampling rate of 64.

It can be observed, that for the same oversampling rate of 8, the demodulated output signal of the Sigma-Delta model with a microphone, results in a much worse signal. This is due to the imperfect characteristics of the

microphone, whose frequency characteristics are far from an integrator. This could, however, be in the future improved with additional compensating analog circuitry. In Figure 3.6, the input analog signal is converted to a digital signal much more accurately, resulting in a better demodulated signal.

Implementing the convolution in a for loop proved to be much more computationally difficult than the general Sigma-Delta model, which was, however, expected. The MATLAB code for this simulation is included in the Appendix B.

Part II

Practical Part

Chapter 4

Hardware Design of a PVDF Sigma - Delta Converter

To test the functionality of the proposed system, a printed circuit board of a PVDF Sigma-Delta converter was designed. This was in order be able to use a transducer supplied by the supervisor in the Sigma-Delta converter. The main objectives of this PCB was to:

- test the functionality of a simple Sigma-Delta converter,
- use SMT components,
- have flexibility to test different components.

4.1 Schematic design

4.1.1 Power Supply

To design the analog circuits, use of a bipolar power supply was chosen. This was, to be able to use the simplest forms of circuits with operation amplifiers and to later use this design together with the pre-amplifier built onto the condenser microphone. A simple approach was chosen - a linear regulator was used to step down the voltage and then create the negative voltage rail with an inverter.

The chosen linear regulator was AZ1117CH-3.3TRG1 by Diodes Incorporated [17].

The main characteristics of AZ1117CH-3.3TRG1 are:

- Minimum input voltage 4.8 V
- Maximum input voltage 10 V
- Maximum output current 1.35 A
- Output voltage: 3.3 V
- Typical line regulation: 0.5 mV

The inverter chosen to create the negative rail was LM2776DBVT by Texas Instruments [18]. The main characteristics, which are important for this design are:

- Minimum input voltage: 2.7 V
- Maximum input voltage: 5.5 V
- Maximum output current: 200 mA
- Output voltage: -Vin
- Switching frequency: 2 MHz

The schematic diagram of the PSU is shown in Figure 4.1.

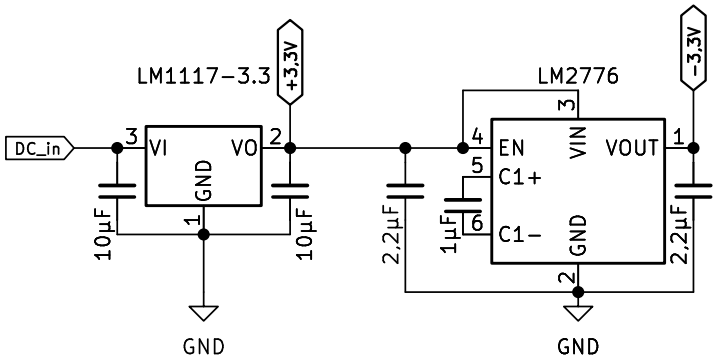

Figure 4.1: Schematic of the designed PSU

4.1.2 Additional Compensating Circuit

An additional compensating circuit utilising a dual operational amplifier OPA1642AID, which is fully specified for audio applications [19], was proposed. Its' main characteristics of OPA1642AID are:

- Minimum operating voltage: ±2.25 V
- Maximum operating voltage: ±18 V
- Input bias current: 2 pA
- Channel quiescent current: 1.8 mA
- THD+N: 0.00005

The proposed schematic can be seen in Figure 4.2. This design is yet to be tested, the actual parts, which were used in the current testing setup, are shown in Figure 4.3.

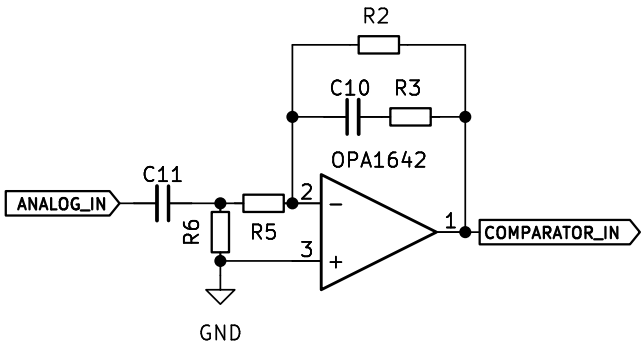

Figure 4.2: Schematic of a proposed compensation circuit

The used circuit, an inverting amplifier, is shown in Figure 4.3 The gain of this block is

$$A_U = -\frac{R_2}{R_5}, \tag{4.1}$$

if we consider the operation amplifier to be ideal.

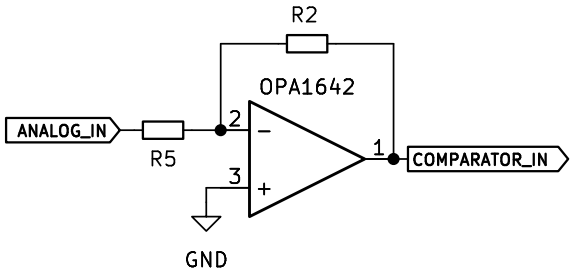

Figure 4.3: Schematic of the used input block - an inverting amplifier

4.1.3 Comparator

A comparator was constructed by using an operational amplifier with positive feedback. The IC is powered from 0 to 3.3 V to ensure, that the output voltage is safe for the D-Latch ICs' input 4.1.4. The designed circuit consists of R_{13} and R_{15} to set the hysteresis of the comparator, but while testing, only a simple comparator, which can be seen in Figure 4.5, was used. This was done by not placing R_{13} and placing an 0 Ω resistor on R_{15}.

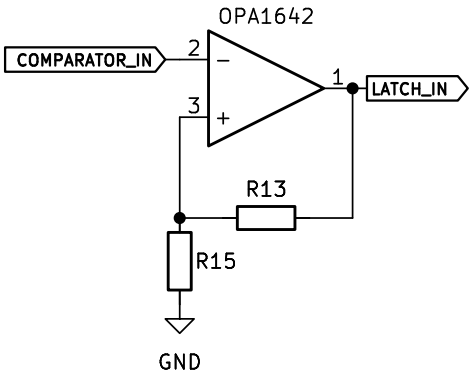

Figure 4.4: Schematic of a proposed comparator with hysteresis

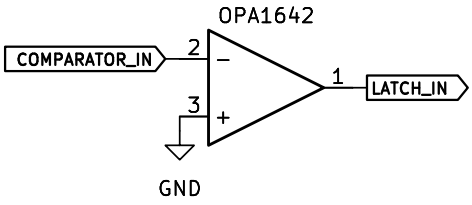

Figure 4.5: Schematic of the implemented comparator block

4.1.4 D-Latch

A D-Latch is an integral part of the Sigma-Delta loop, which synchronizes the digital output with an incoming clock. To do that, MC74HC74ADG by ON Semiconductor was chosen. It is a Dual D Flip-Flop with Set and Reset [20]. The main characteristics of MC74HC74ADG are:

- Minimum operating voltage: 2 V
- Maximum operating voltage: 6 V
- Input bias current: 2 pA
- Maximum clock frequency: 4.8 MHz
- THD+N: 0.00005

The schematic of the D-Latch block can be seen in Figure 4.6

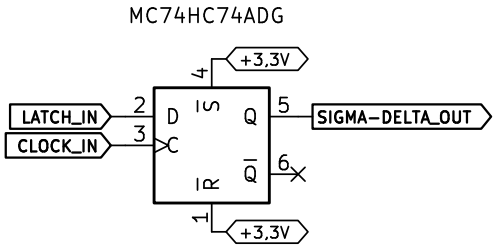

Figure 4.6: Schematic of the D-Latch block

The function table of this IC is shown in Figure 4.7 [20].

FUNCTION TABLE

Inputs				Outputs	
Set	Reset	Clock	Data	Q	$\overline{Q}$
L	H	X	X	H	L
H	L	X	X	L	H
L	L	X	X	H*	H*
H	H	↑	H	H	L
H	H	↑	L	L	H
H	H	L	X	No Change	
H	H	H	X	No Change	
H	H	↓	X	No Change	

Figure 4.7: D-Latch function table [20]

The output of the D-Latch shown in Figure 4.6 is the Sigma-Delta or PDM signal. To create a differential block, this signal needs to be inverted and amplified to be sent into the PVDF membrane.

4.1.5 Output Circuitry

The PVDF output circuitry shown in Figure 4.8 consists of an inverting amplifier, where the gain of this block is

$$A_U = -\frac{R_4}{R_{10}}. \tag{4.2}$$

While testing, the gain was set to be $A_U = -1$, which ensures, that the circuit uses its' biggest possible voltage range.

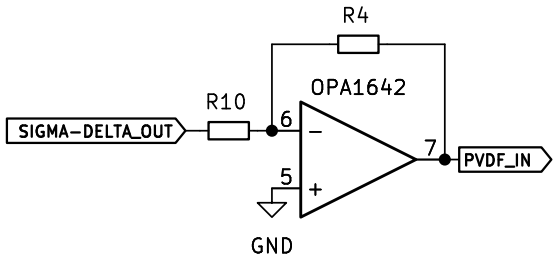

Figure 4.8: Inverting Output Amplifier Schematic Diagram

4.2 PCB design

All of the subcircuits discussed in 4.1 were implemented in KiCad EDA software on an experimental printed circuit board. All of the files - including a schematic diagram, PCB design and final GERBER files, can be found in Appendix B.

The circuit was designed for a double sided PCB made from FR4 material. The top copper and silkscreen design can be seen in Figures 4.9 and 4.10. The design of the bottom layer can be seen in Figures 4.11 and 4.12.

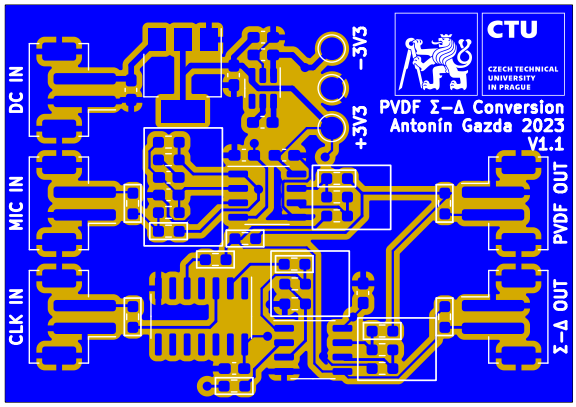

Figure 4.9: Top 2D view of the designed PVDF Sigma-Delta converter PCB

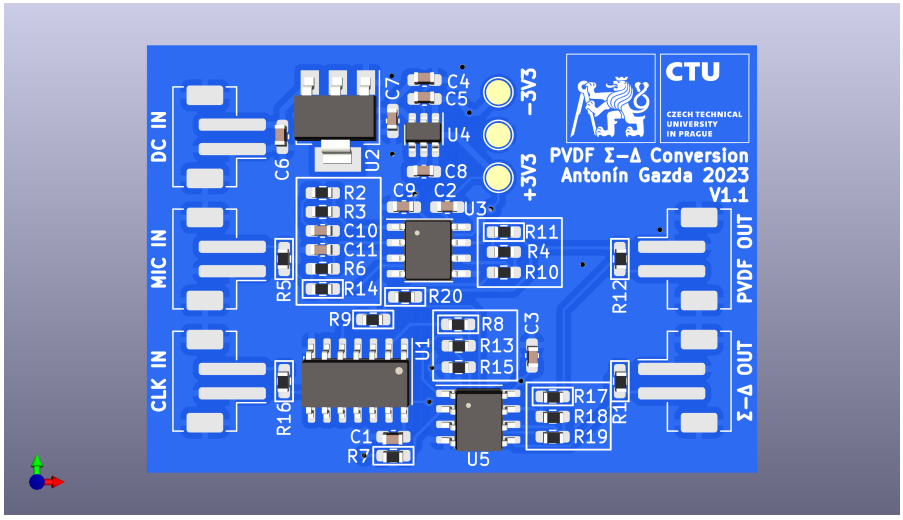

Figure 4.10: Top 3D view of the designed PVDF Sigma-Delta converter PCB with components

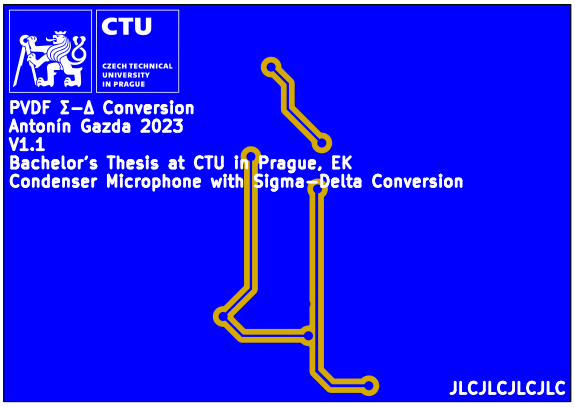

Figure 4.11: Bottom 2D view of the designed PVDF Sigma-Delta converter PCB

Figure 4.12: Bottor 3D view of the designed PVDF Sigma-Delta converter PCB with components

Chapter 5
Hardware Testing

5.1 Demodulation

A digital signal processor (DSP) was used to demodulate the PDM signal. The selected processor was ADAU1452 by Analog Devices [21] with impemented circuitry on an EVAL-ADAU1452REVBZ evaluation board [22]. The processor was programmed in Sigma Studio - a *graphical development tool for programming, development, and tuning software for ADI DSP audio processors and A2B® transceivers* by Analog Devices [23]. A photo of this evaluation board can be seen in Figure 5.2.

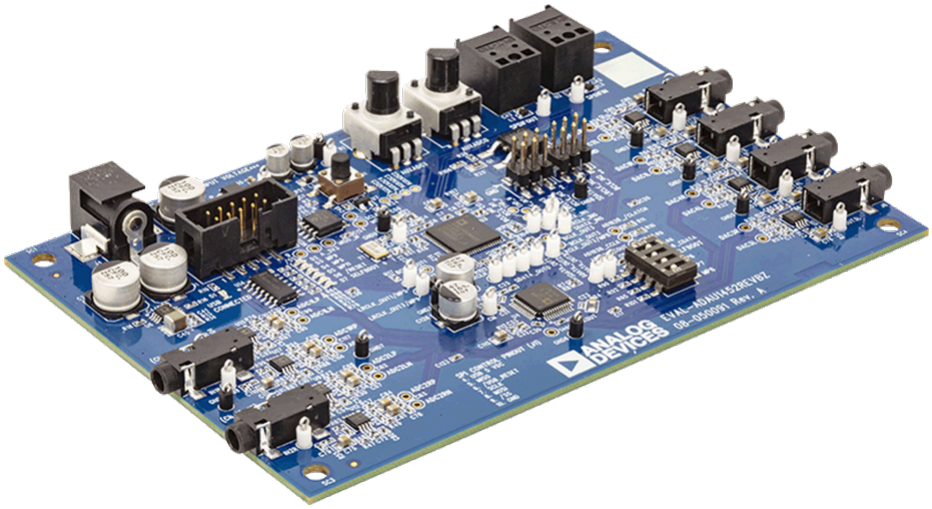

Figure 5.1: Photo of an EVAL-ADAU1452REVBZ Board

First, a connection to the DSP IC needed to be established by connecting the evaluation board to an USB SPI interface. This was done by creating the schematic seen in Figure 5.2.

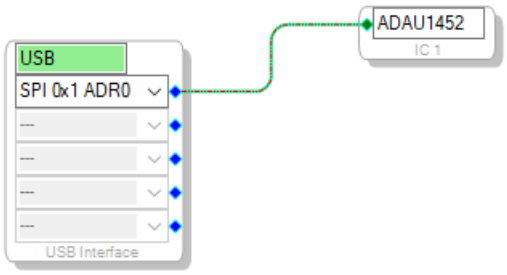

Figure 5.2: Sigma Studio USB Connection Schematic

A block schematic shown in Figure 5.3 was created by connecting a DigMicIn module, which contains up to 4 digital microphone outputs, to an output block. The signal from the DigMicIn block is automatically demodulated.

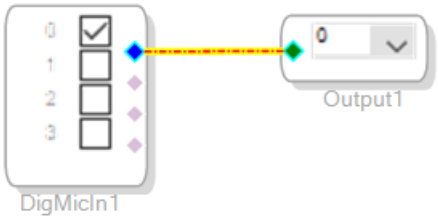

Figure 5.3: Sigma Studio Digital Microphone Schematic

A DMIC CTRL0 register [21] needed to be set up to use a data source on pin MP12 and clock Input BCLK2. The register settings can be seen in Figure 5.4. Moreover the MP12 MODE register was set up to register the signal as digital microphone input. This setting can be seen in Figure 5.5. The Sigma Studio project is also included in the Appendix B.

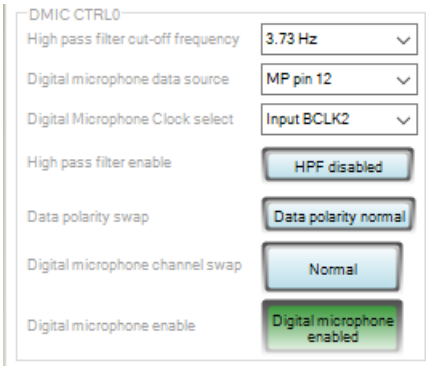

Figure 5.4: DMIC CTRL0 Register Setup

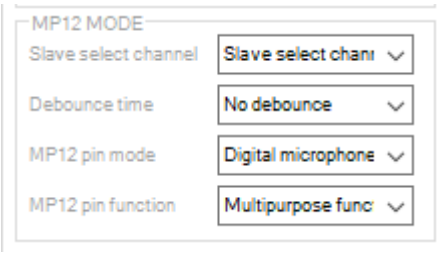

Figure 5.5: Sigma Studio Pin Mode Setup

To test the functionality of the PDM demodulation, a MEMS PDM microphone SPH0641LU4H-1 by Knowles [24] was connected to the programmed DSP evaluation board. The resulting demodulated signal of a clap was displayed on an oscilloscope is shown in Figure 5.6.

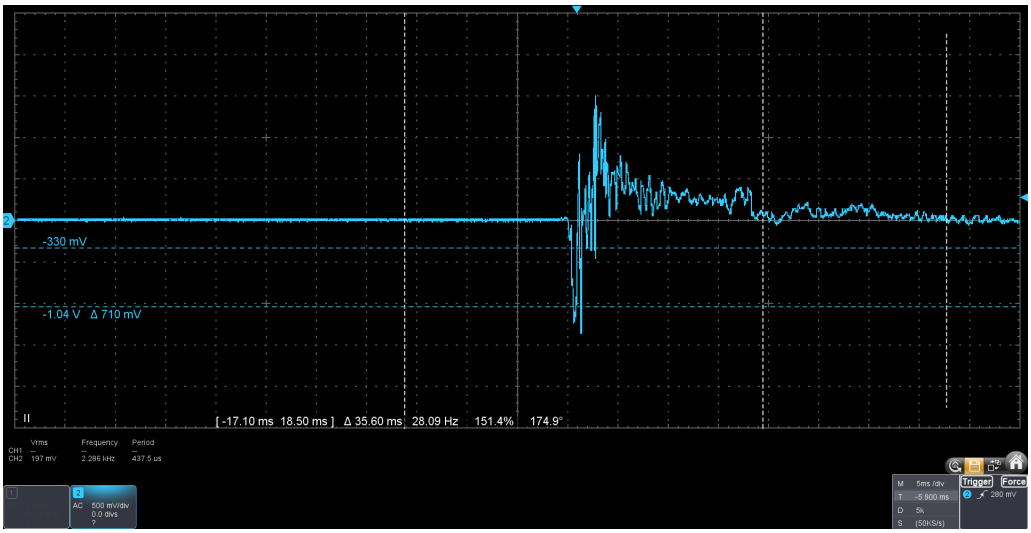

Figure 5.6: Demodulated signal from SPH0641LU4H-1

5.2 Testing Setup

A testing setup was created to evaluate the functionality of the system. The testing diagram can be seen in Figure 5.7.

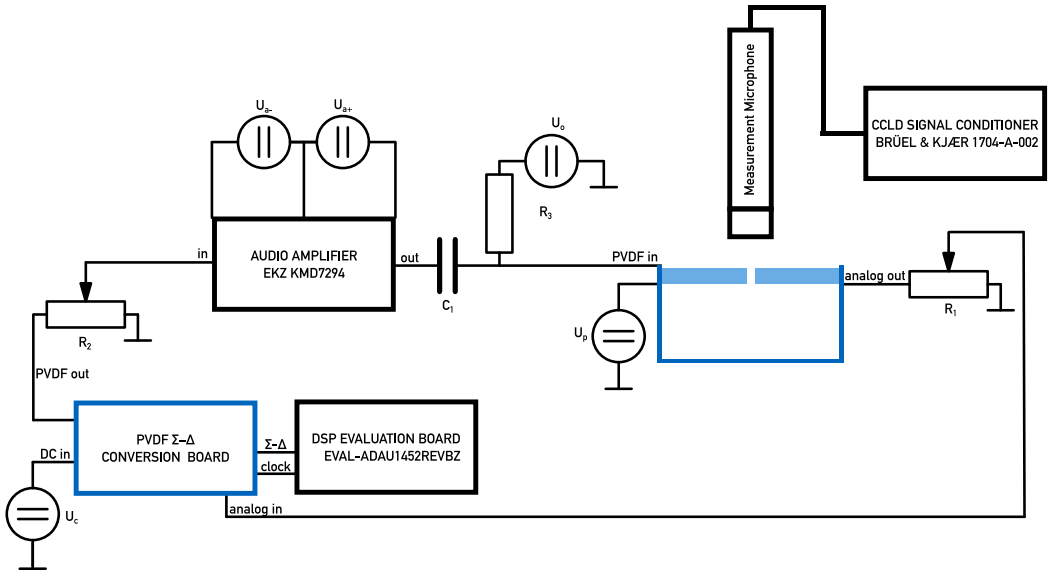

Figure 5.7: A diagram of the final testing setup

A condenser microphone provided by the supervisor is made up of a static electrode with an integrated pre-amplifier and a piezoplastic membrane. The pre-amlifiers' circuitry is powered by a 9 V battery U_b.

The polarisation for the condenser microphone provided by an external high voltage power supply U_p. The voltage was measured to be 165 V.

The microphone was tested, that it functions correctly. One of the weak spots of the design is the operational amplifier located on the microphones' static electrode, which is prone to being destroyed, if the membrane accidentally touches the electrode.

The analog output of the microphone was attenuated with a potentiometer R_1. This signal is the input for the custom made PVDF Sigma-Delta Conversion Board. The conversion boards' circuitry is powered by U_c

A DSP Evaluation Board programmed to output a clock signal and demodulate incoming Sigma-Delta is connected to the PVDF Conversion Board. The DSP is powered by an external voltage source U_d.

The PVDF output from the conversion board gets attenuated by R_2.

To achieve higher maximum amplitude of the PVDF signal, an audio amplifier was used. The amplifier is powered by U_{p+} and U_{p-}. Because this amplifier is designed for audio signals, it only outputs signals without DC offset, which was then added by connecting U_o through a resistor R_3.

This signal, which can achieve from 0 to -70 V is sent into the PVDF membrane.

Because of the low sensitivity of the PVDF membrane, the digital signal

sent into the PVDF doesn't affect the resulting signal very significantly even at an amplitude of 70 V.

In Figure 5.8, it can be seen, that a signal of amplitude 66 V sent into the PVDF, results in only about 20 mVpp at the output of the microphone.

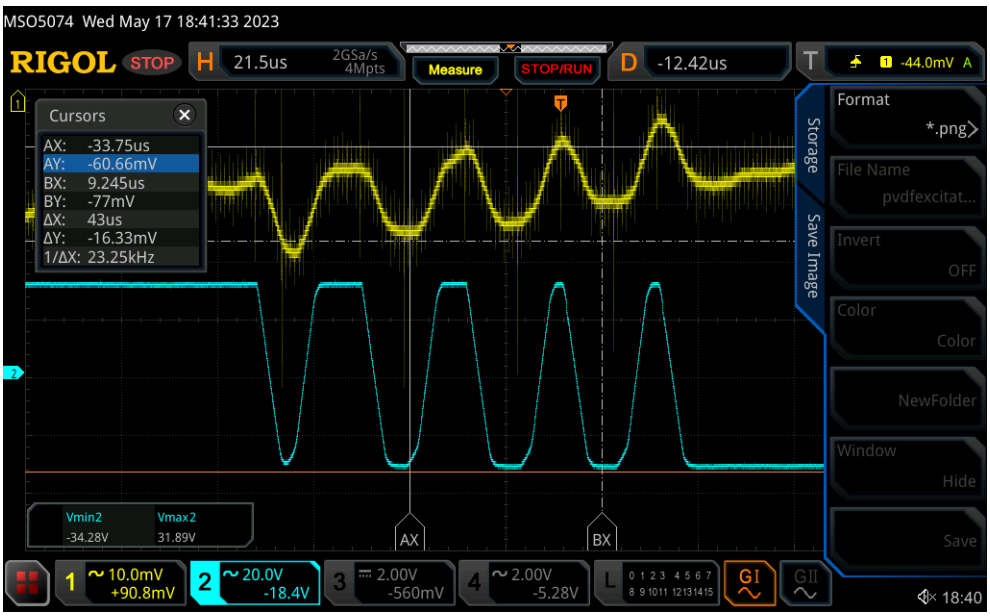

Figure 5.8: PVDF membrane excitation input (blue curves) and microphone analog output (yellow curves)

At a sampling rate of 8 kHz, the current functionality of the system can be seen in Figure 5.9.

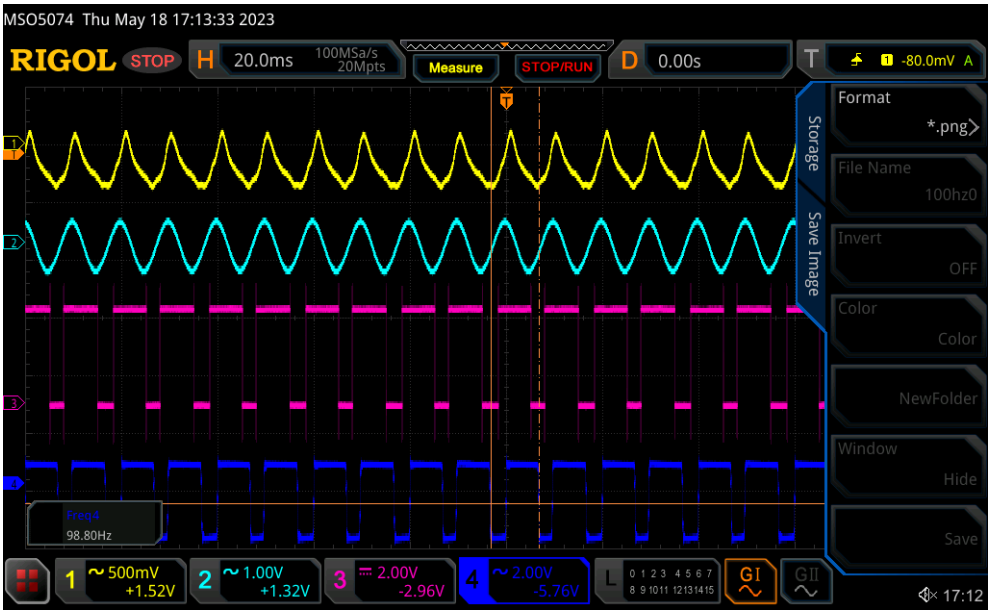

Figure 5.9: 8 kHz Sampling Rate 100 Hz Sinewave Modulation - microphone output (yellow curves), acoustic pressure input (aqua curves), Sigma-Delta output (magenta curves), demodulated signal (blue curves)

A closer view at the constructed signal can be seen in Figure 5.10, a close up of the signal.

Figure 5.10: 8kHz Sampling Rate 100 Hz Sinewave Modulation Close Up - microphone output (yellow curves), acoustic pressure input (aqua curves), Sigma-Delta output (magenta curves), demodulated signal (blue curves)

A model of the Sigma-Delta loop was modified for the PVDF to affect the microphones' output. It is shown in Figure 5.11. The Sigma-Delta output

results in much less data, and the demodulated signal can be seen to be much more similar to a square wave of the measured input signals' frequency. This shows, that there is a possibility of improving the functionality by amplifying the signal sent to the PVDF membrane. This could be done by utilising a better suited amplifier (as the 1-bit DAC block) or by redesigning the output circuitry - for example using a MOSFET to switch an high voltage external voltage source.

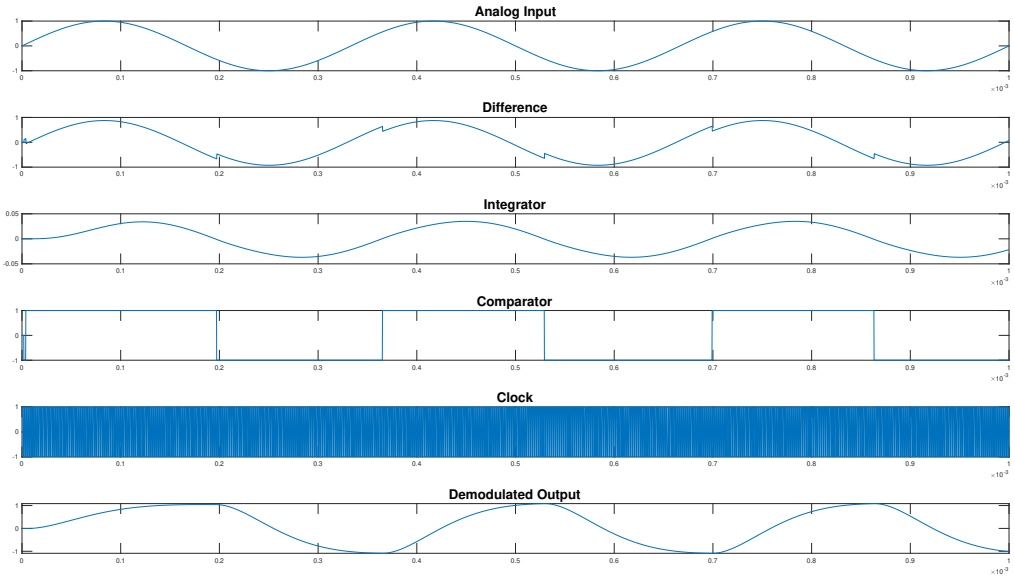

Figure 5.11: Modeled Sigma-Delta diagram with dampened PVDF amplitude

The same measurement was done for a sampling rate of 192 kHz. The amount of data in the Sigma-Delta signal increases. This can be seen in Figures 5.12 and 5.13.

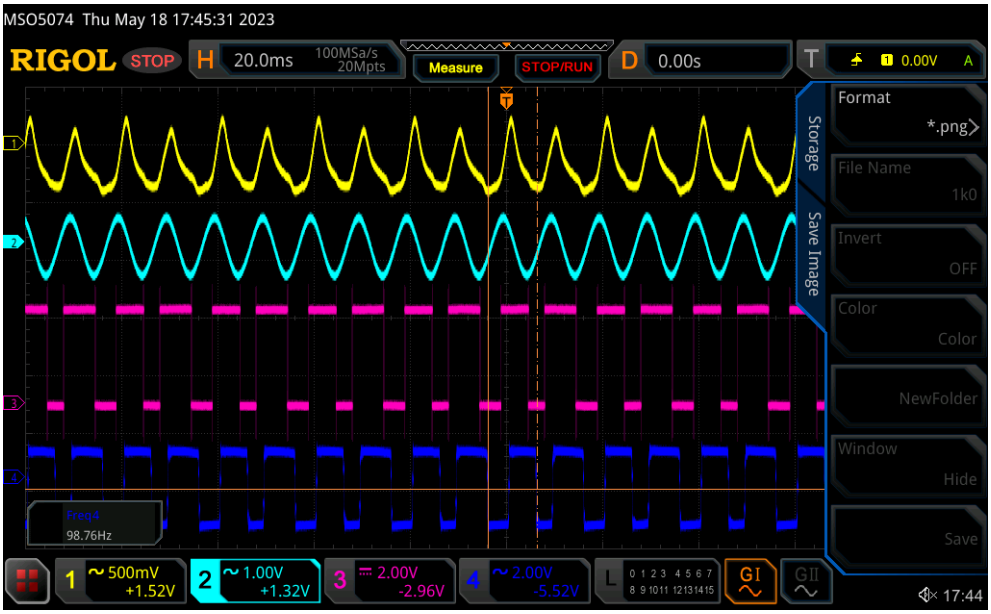

Figure 5.12: 192kHz Sampling Rate 100Hz Sinewave Modulation

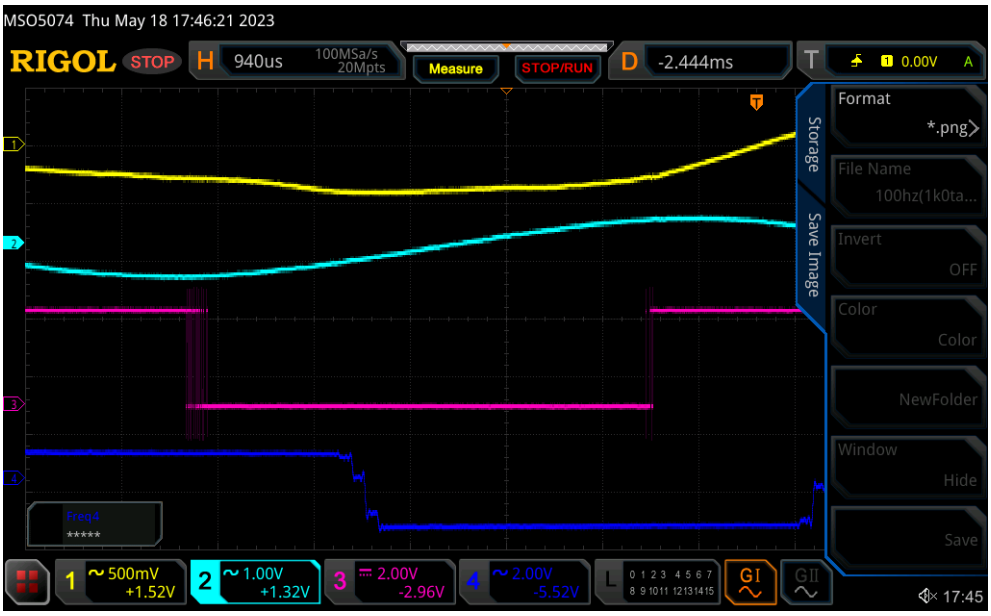

Figure 5.13: 192kHz Sampling Rate 100Hz Sinewave Modulation Closeup

Conclusion

In this thesis, basic principles of condenser microphones were discussed. Moreover, the foundation for creating an equivalent circuit model of a condenser microphone was described.

An equivalent circuit model of a condenser microphone was implemented in MATLAB and compared to a more precise numerical model. The equivalent circuit model was deemed to be correctly implemented and precise enough for this application.

The equivalent circuit model was used to simulate an impulse response of the microphone, to be able to simulate the microphones' characteristics in the time domain.

A generic first order Sigma-Delta loop model was implemented and then adjusted to be able to use the modeled impulse response to simulate how the proposed microphone in the Sigma-Delta loop could be used.

A hardware schematic and a printed circuit board for a PVDF conversion block was designed and subsequently manufactured.

The PVDF Sigma-Delta conversion board was tested and evaluated.

It was determined, that the proposed system for converting analog acoustic pressure directly to a digital signal could be viable, if edits were made in the design to be able to excite the PVDF membrane in a way, which would result in higher response in the analog output of the microphone. Alternatively, an electrostatic excitation of the membrane could be tested.

Bibliography

[1] ŠKVOR, Zdeněk. *Akustika a elektroakustika.* Praha: Academia, 2001. ISBN 80-200-0461-0.

[2] KADLEC, František. *Zpracování akustických signálů.* Praha: Vydavatelství ČVUT, 1996. ISBN 80-01-01525-4.

[3] JIŘÍČEK, Ondřej. *Úvod do akustiky.* Praha: Vydavatelství ČVUT, 2002. ISBN 8001024801.

[4] BEIS, Uwe, *An Introduction to Delta Sigma Converters* website [online]. 2020, [quot. 2023-06-24]. Available from: https://www.beis.de/Elektronik/DeltaSigma/DeltaSigma.html

[5] L. L. Beranek, T. J. Mellow, *Acoustics, Sound Fields and Transducers*, Elsevier, Oxford, 2012

[6] Škvor, Z.: *Vibrating Systems and their Equivalent Circuits*, Elsevier, Amsterdam, 1991.

[7] Estèves, J., Rufer, L., Ekeom, D., Basrour, S., Lumped-parameters equivalent circuit for condenser microphones modeling, *J. Acoust. Soc. Am.* **2017**, *142*, 2121–2132.

[8] K. Abramova, P. Honzík *Experimental Estimation of Unknown Parameters of Equivalent Circuits of Low-cost Electret Microphones*, Akustické listy, 23(1–4), December 2017.

[9] Zuckerwar A. J.: Theoretical response of condenser microphones, *J. Acoust. Soc. Am.***64**(5), 1278-1285 (1978).

[10] M. Bruneau, A.-M. Bruneau, Z. Škvor, and P. Lotton, "An equivalent network modelling the strong coupling between a vibrating membrane and a fluid film," Acta Acust. Acust. 2, 223–232 (1994).

[11] T. Lavergne, S. Durand, M. Bruneau, and N. Joly, Analytical Modeling of Electrostatic Transducers in Gases: Behavior of Their Membrane and Sensitivity, Acta Acust. united Ac., **100** (2014), 440-447.

[12] N. Joly, “Finite Element Modeling of Thermoviscous Acoustics on Adapted Anisotropic Meshes: Implementation of the Particle Velocity and Temperature Variation,” Acta Acust. united Ac. **96**(1), 102-114 (2010).

[13] N. Joly, M. Bruneau, R. Bossart “Coupled Equations for Particle Velocity and Temperature Variation as the Fundamental Formulation of Linear Acoustics in Thermo-Viscous Fluids at Rest,” Acta Acust. united Ac. **92**, 202-209 (2006).

[14] Acoustics Module User’s Guide, COMSOL (2015).

[15] W. R. Kampinga, Y. H. Wijnant, A. de Boer “An Efficient Finite Element Model for Viscothermal Acoustics,” Acta Acust. united Ac. **97**, 618-631 (2011).

[16] M. J. Herring Jensen, E. Sandermann Olsen, "Virtual prototyping of condenser microphone using the finite element method for detailed electric, mechanic, and acoustic characterisation," Proceeding of Meetings on Acoustics **19**, 030039, (2013).

[17] Diodes Incorporated, *AZ1117C* datasheet [online]. 2019, [quot. 2023-06-24]. Available from: https://cz.mouser.com/datasheet/2/115/DIOD_S_A0007713706_1-2542909.pdf

[18] Texas Instruments, *LM2776* datasheet [online]. 2021, [quot. 2023-06-24]. Available from: https://www.ti.com/lit/ds/symlink/lm2776.pdf

[19] Texas Instruments, *OPA164x* datasheet [online]. 2022, [quot. 2023-06-24]. Available from: https://www.ti.com/lit/ds/symlink/opa1641.pdf

[20] ON Semiconductor, *MC74HC74A* datasheet [online]. 2022, [quot. 2023-06-24]. Available from: https://cz.mouser.com/datasheet/2/308/MC74HC74A_D-1280823.pdf

[21] Analog Devices, *ADAU1452* datasheet [online]. 2014, [quot. 2023-06-24]. Available from: https://www.analog.com/media/en/technical-documentation/data-sheets/ADAU1452.pdf

[22] Analog Devices, *EVAL-ADAU1452REVBZ User Guide* datasheet [online]. 2019, [quot. 2023-06-24]. Available from: https://www.analog.com/media/en/technical-documentation/user-guides/EVAL-ADAU1452REVBZ-UG-1662.pdf

[23] Analog Devices, *Sigma Studio* website [online]. 2023, [quot. 2023-06-24]. Available from: https://www.analog.com/en/design-center/evaluation-hardware-and-software/software/ss_sigst_02.html

[24] Knowles, *SPH0641LU4H-1* datasheet [online]. 2014, [quot. 2023-06-24]. Available from: https://cz.mouser.com/datasheet/2/218/know_s_a0010889928_1-2271691.pdf

Appendices

Appendix A

List of abbreviations

Abbreviation	Meaning
3D	3-dimensional
A/D	Analog to Digital
A2B	A2B Audio Bus
ADI	Analog Devices
DC	Direct Current
DSP	Digital Signal Processor
FEM	Finite Element Method
IC	Integrated Circuit
LTI	Linear Time-Invariant System
MEMS	Micro Electro Mechanical System
PCB	Printed Circuit Board
PDM	Pulse-Density Modulation
PSU	Power Supply Unit
PVDF	Polyvinylidene Fluoride
SMT	Surface Mount Technology
SNR	Signal to Noise Ratio
SPI	Serial Peripheral Interface
THD+N	Total Harmonic Distortion Plus Noise
USB	Universal Serial Bus

Appendix B

Included files

- KiCad
  - SigmaDeltaV3
    - plots
      - SigmaDeltaV3-B_Cu.svg
      - SigmaDeltaV3-B_Silkscreen.svg
      - SigmaDeltaV3-Edge_Cuts.svg
      - SigmaDeltaV3-F_Cu.svg
      - SigmaDeltaV3-F_Silkscreen.svg
      - SigmaDeltaV3-Schematic.pdf
    - production
      - bom.csv
      - SigmaDeltaV3_GERBERS.zip
    - SigmaDeltaV3.kicad_pcb
    - SigmaDeltaV3.kicad_pro
    - SigmaDeltaV3.kicad_sch
- MATLAB
  - Equivalent-Circuit-Model
    - png
      - Model.png
      - ModelDifferentCavityThicknesses.png
      - ModelDifferentGapLengths.png
      - ModelDifferentMeasuredResonantFrequencies.png
      - ModelDifferentMembraneRadii.png
    - besselzero.m
    - calculateSimpleCircuitModel.m
    - plotMyData.m
    - simulate.m
  - Sigma-Delta-Model
    - besselzero.m
    - calculateSimpleCircuitModel.m
    - generateImpulseResponse.m
    - simulate.m
- SigmaStudio
  - PDM_Demodulation_ADAU1452.dspproj